Journal of Nepal Geological Society, 2008, Vol. 38, pp. 39–48

Magnetic fabric of Siwalik sediments (Nepal): implications to time–space evolution of stress field

Pitambar Gautam

Creative Research Initiative "Sousei", Hokkaido University, N21 W10 Sapporo 001-0021, Japan
(Email: pgautam2000@yahoo.com)

ABSTRACT

Magnetic fabric data based on the anisotropy of magnetic susceptibility (AMS) of the sediments constituting the Siwalik sections (Karnali R., Amilia–Tui Road, Surai R., Tinau R., and Rato R.) in Nepal have been analysed for the variability of magnetic lineation and the implications to the time-space evolution of the stress field in this region during the last 16 myrs. This involved compilation of (i) the magnetic polarity data that constrain the depositional age of the Nepalese Siwaliks to ca. 16 to 1 Ma, and (ii) the declination of characteristic magnetic remanence to reveal the relative tectonic rotations (17° CCW at Butwal to 9° CW at Amilia). The magnetic fabric, defined mainly by alignment of paramagnetic minerals, corresponds to an oblate ellipsoid with foliation parallel to bedding plane, implying a sedimentary-compactional origin. The magnetic lineations show well defined clusters (confined in or close to the bedding plane). Being subparallel to the fold axes/bedding strikes/thrust fronts, these lineations are assumed to originate from a secondary mild deformation process related to the compression tectonics in the Siwalik foredeep and therefore correspond to the active direction of the minimum principal horizontal stress active during foredeep deposition. Hence, the direction of compression is orthogonal to the mean lineation. The compression direction in the palaeogeographic coordinates can be obtained by introducing an additional correction for the tectonic rotation about the vertical, using the palaeomagnetic declination. Available AMS-based lineations, corrected for rotation about vertical using palaeomagnetic declinations, reveal that the compression direction in the Himalayan foreland remained in general N to NNE with significant deviations in its far western part, in particular around the Amilia–Tui section where the direction was N58°E.

Keywords: Magnetic polarity, magnetostratigraphy, magnetic fabric, anisotropy of magnetic susceptibility, Siwaliks, foreland basin, oblate fabric, stress field, Nepal

Received: 22 December 2006; **revision accepted:** 26 March 2008

INTRODUCTION

Magnetostratigraphy of the Siwalik sediments in the Nepalese foreland basin has constrained the depositional age between ca. 16 to 1 Ma and yielded declination anomalies indicative of tectonic rotations of the various segments along the Siwalik range (Appel et al. 1991; Gautam and Appel 1994; Rösler et al. 1997; Rösler and Appel 1998; Gautam and Rösler 1999; Ojha et al. 2000; Gautam and Fujiwara 2000). In addition, several sections have been studied for the magnetic fabric using the anisotropy of magnetic susceptibility (AMS) (Gautam and Pant 1996; Gautam and Rösler 1999). The magnetic datasets acquired from the Nepalese Siwaliks indicate a significant variability by section in terms of age span, lithology, rates of sediment accumulation with age and the magnetic fabric (anisotropy parameters, lineation, foliation etc.). This is to be expected because the sediment-fill of the former foreland basin results from a complex interaction of tectonic and climatic events dictated by the role played by various processes, such as collision-induced crustal thickening, growth of the thrust wedge, the isostatic adjustments of the cratonic lithosphere to thrust loading, the surface processes that redistribute material from the mountain belt into the surrounding basins, the geometry of individual basins, and the hydraulic regime (cf. Huyghe et al. 2005 and references therein).

The objective of this paper is to present a summary of the magnetostratigraphic and magnetic anisotropy data, and thereby make these data more accessible for interpretation of local or regional tectonic and climatic inferences in the Siwalik basin and the source areas in the main Himalayan region. Emphasis in this paper is given to the interpretation of the AMS-based magnetic lineation to infer the palaeocompression direction along the Himalayan arc as an aid to seismotectonic study.

MAGNETIC POLARITY STRATIGRAPHY

Since the previous compilation of the magnetic polarity sequences (Gautam and Rösler 1999), additional data were published from several sections: Karnali R. (Gautam and Fujiwara 2000), Khutia R. (Ojha et al. 2000), and Surai (renewed sampling: Hoorn et al. 2000). A renewed compilation

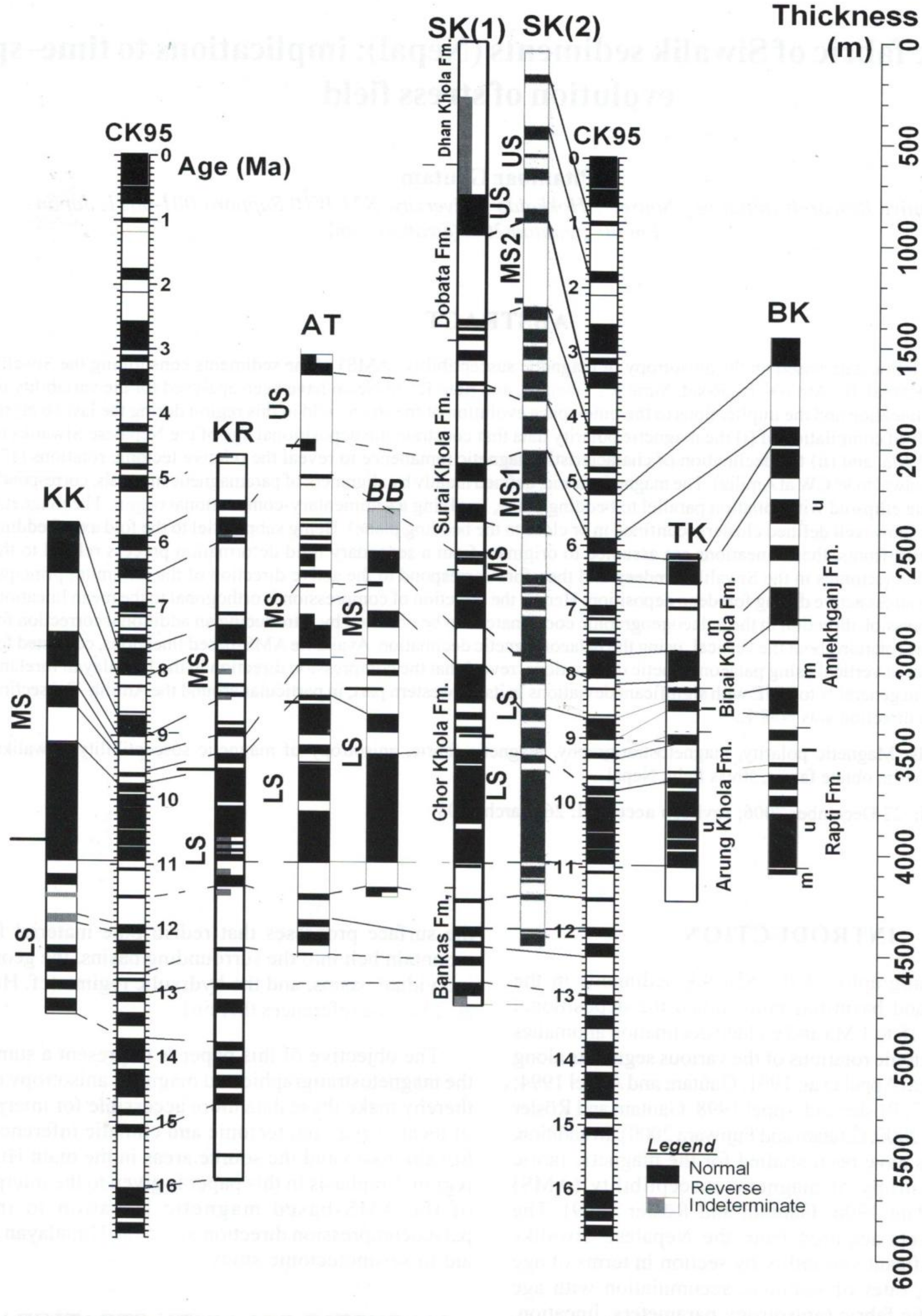

Fig. 1: Compilation of magnetic polarity sequences established for the Siwalik sediments in Nepal. Abbreviations for sections (from east to West) and data sources are as follows. BK: Bakiya Khola (= river) (Harrison et al. 1993); TK: Tinau Khola (Gautam and Appel 1994); KK: Khutia Khola (Ojha et al. 2000); SK: Surai Khola (SK1: Rösler et al. 1997; SK2: Hoorn et al. 2000); BB: Bhalubang (Rösler et al. 1997); AT: Amilia–Tui (Rösler et al. 1997); KR: Karnali River (Gautam and Fujiwara 2000); and KK: Khutia Khola (Ojha et al. 2001). CK95 used as standard geomagnetic polarity time scale for calibration is after Cande and Kent (1995). Locations of these sections are shown in the generalised geological map in Fig. 5.

is hence shown in Fig. 1. The total thickness of the Siwalik section is assumed to be ca. 6000 m. To facilitate comparison, the base of the long normal polarity Chron 5n, which is the most reliably determined part of the polarity sequence, is placed at the same level, for all sections in the compiled diagram. The compilation shows that the Karnali section contains the oldest rocks (> 16 Ma) where ca. 100 m or thicker poorly exposed section at the base remains yet undated.

The youngest age assigned is <1 Ma for the topmost dated portion of the Surai Khola section. The diagram shows another fact that there is no general consensus among the researchers working in the Siwaliks regarding the placement of the boundaries between the traditional divisions (Lower Siwaliks: LS; Middle Siwaliks: MS; Upper Siwaliks: US); the divisions shown along each sections are as they appear in the works of respective authors. Therefore, it is impossible to assign an age to the LS–MS or MS–US boundaries without disregard to the section concerned (Gautam and Fujiwara 2000). For the Nepalese Siwaliks, in the absence of index fossils that could give depositional ages and lack of findings of any volcanic ash layers (which do occur in the Indian and Pakistani Siwaliks and yield absolute ages by fission track dating; e.g. volcanic ash or tuff deposits within the Nagri Formation and Jalalpur section in Pakistan, dated respectively at 9.5±0.63 Ma and 2.53±0.35; see Johnson et al. 1982), magnetostratigraphy is the sole tool used for age assignment.

SEDIMENT ACCUMULATION RATES

Fig. 2 is a compilation of the sediment accumulation rate (SAR) estimates from the polarity sequences presented in Fig. 1. Although lithofacies variations and decompaction have not been considered, this compilation is believed to give a regionally-averaged picture. From the curves, the variability in SARs among various sections is obvious. The average bar diagram reveals 2 distinct highs in SARs: (i) from 10.9 to 9.7 Ma (time span of chron C5n); and (ii) from 5.2 to 3.6 Ma (time span of chrons C2Ar to C3n4.n).

According to Molnar (2005), a significant dataset on the environmental changes in the Himalaya–Tibet region can be related to 7–8 Ma or near that time. This time is commonly related to the intensification of the Asian monsoon. Detailed sedimentological studies (Tokuoka et al. 1986, Dhital et al. 1995) and facies analyses (Tanaka 1997; Nakayama and Ulak 1999; Ulak and Nakayama 2001; Huyghe et al. 2005) of several sections of the Nepalese Siwaliks sections provide data on evidence for the presence of material derived from the Higher Himalayan Crystallines (HHC) and initiation of flood-flow-dominated meandering system during ca. 12.5–9.0 Ma (the differences in timing being probably dependent on a multitude of factors such as catchment area, surface topography, tectonics) attributable to an increase in precipitation in relation to probable initiation of monsoon. The facies corresponding to the flood-flow-dominated system include rather thick, up to 10 m, medium to coarse sandstones which contain the material derived from the HHC. Hence, the maximum SAR for 10.9 to 9.7 Ma age range are likely to reflect a combined response of the uplift of the main HHC and its subsequent erosion in concert with genetically related monsoon precipitation in its initial stage and (or) subsidence of the Siwalik depositional basin.

MAGNETIC FABRIC BASED ON ANISOTROPY OF MAGNETIC SUSCEPTIBILITY (AMS)

The magnetic fabric of several Siwalik sections has been established on the basis of AMS parameters, details of which were given in Gautam and Rösler (1999) and Gautam et al. (2000). It is contributed primarily by paramagnetic minerals as shown by rather low bulk susceptibility magnitudes clustering around 10^{-4} SI (see Rochette et al. 1992). It has mainly oblate shape, with parallelism of bedding-tilt corrected magnetic foliation with the bedding planes or subvertical nature of the bedding-tilt corrected magnetic susceptibility minimum directions (the poles to magnetic foliation), indicative of a sedimentary-compactional origin. The magnetic lineations, defined by maximum magnetic susceptibility

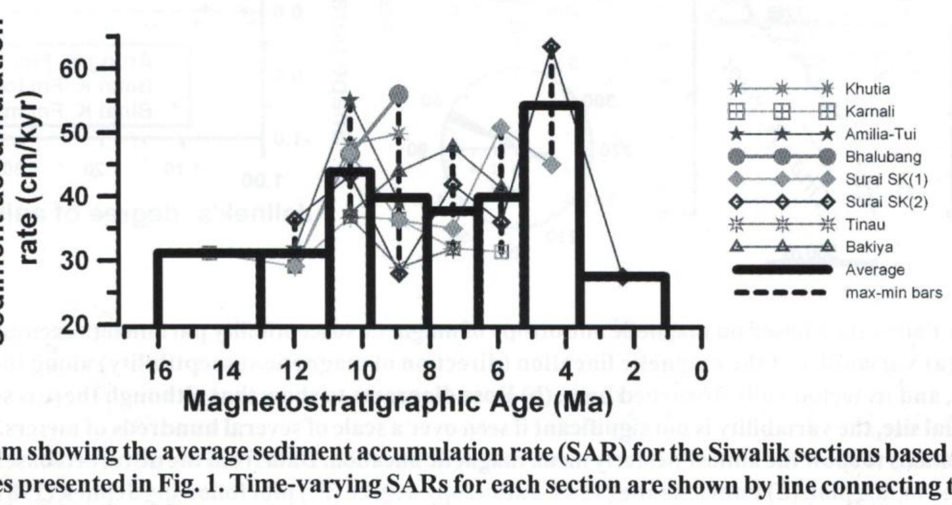

Fig. 2: Bar diagram showing the average sediment accumulation rate (SAR) for the Siwalik sections based on the magnetic polarity sequences presented in Fig. 1. Time-varying SARs for each section are shown by line connecting the mean for the time occupied by the base of each bar.

directions obtained after bedding-tilt correction, show well defined clusters (confined in or close to the bedding plane or palaeohorizontal). The magnetic fabric is represented by mainly oblate susceptibility ellipsoids with a low anisotropy degree (with a few exceptions, P'<1.2; Fig. 3d). The directional consistency of magnetic lineation throughout a representative section, the pre-folding nature as well as the shape versus anisotropy degree have been illustrated in the example of the Tinau Khola section in Fig. 3.

Reasonable directional consistency of the bedding-tilt corrected magnetic lineations is observed throughout the whole duration in each measured section. Also these lineations are almost perpendicular or at high angles to palaeocurrents, inferred from sedimentary structures as SSE to SSW directed (Tokuoka et al. 1986, 1990; DeCelles et al. 1998). The bedding-tilt corrected magnetic lineations are found to be subparallel to the fold axes, bedding strikes, or thrust fronts. Such behaviour of the magnetic fabric resembles to that found in compressive tectonic settings of young mountain belts elsewhere (e.g. Sagnotti et al. 1999; Lee et al. 1990; Gautam et al. 2000 and references therein). A detailed discussion on such pre-folding magnetic fabric in two fold-and-thrust belts is given in Robion et al. (2007). In analogy to the previous studies in various compressive settings, in this study, the magnetic lineation is assumed to result from compression over the duration of sedimentation in the Siwalik foredeep and thus to be parallel to the direction

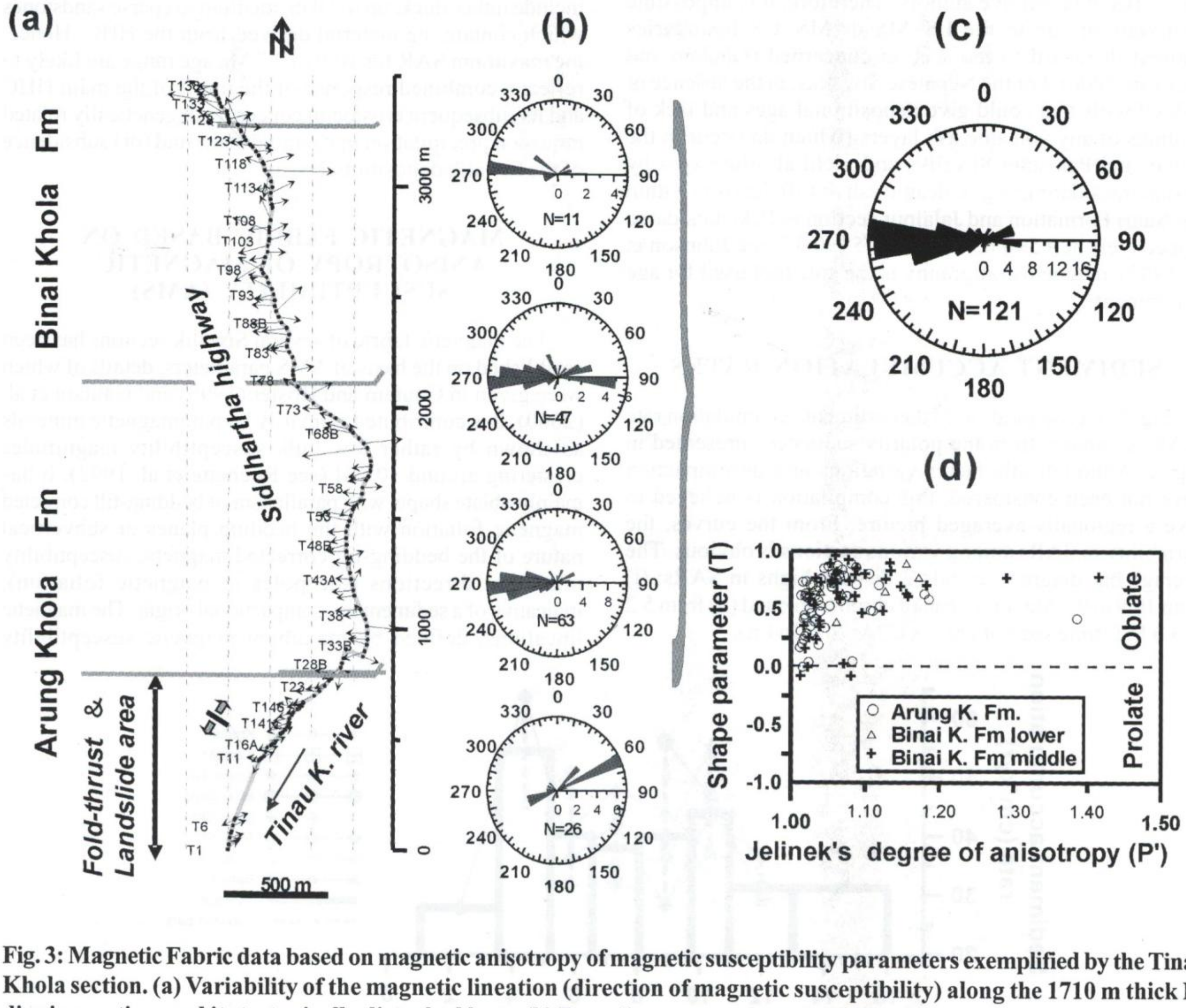

Fig. 3: Magnetic Fabric data based on magnetic anisotropy of magnetic susceptibility parameters exemplified by the Tinau Khola section. (a) Variability of the magnetic lineation (direction of magnetic susceptibility) along the 1710 m thick N-dipping section, and its tectonically disturbed base. (b) Rose diagrams to show that although there is some scatter at the scale of individual site, the variability is not significant if seen over a scale of several hundreds of meters. (c) Rose diagram of magnetic lineations to show the almost westerly mean magnetic lineation. Data from the disturbed base of the section have not been included in this plot. (d) Fabric shape (T) vs. anisotropy degree (P') plot following Jelinek (1981) showing mainly oblate fabric with a low degree of anisotropy.

of the minimum principal horizontal stress active during foredeep deposition. Therefore, the direction of compression derived here is orthogonal to the azimuth of the mean lineation, in palaeogeographic coordinates, in each section or its sectors covered by differing time span.

COMPILATION OF DIRECTIONAL (REMANENCE AND AMS) DATA

Remanent magnetisation directions from individual Siwalik sections reveal the presence of tectonic rotations (about the vertical) at local or regional scale as shown by deviations of the magnetic declinations from the geographic north. Therefore, to get the compression direction from magnetic lineation in the palaeogeographic coordinates, it is necessary to introduce an additional correction using declination data; while using this approach, it is explicitly assumed that lineation development preceded rotation. Moreover, the mean remanence direction, the resulting amount of rotation, as well as the mean lineation are likely to differ according to the time span covered by a particular section. To overcome this, both the remanence and magnetic lineation data have been analysed with respect to several geological age categories (Middle Miocene, Late Miocene, and Pliocene). The compiled data are given in Table 1. Remanence data reveal that the sections in the far west (Khutia and Karnali) and in the centre (Tinau) show anticlockwise rotations whereas the Amilia–Tui and Surai sections exhibit clockwise rotations.

Fig. 4 shows the differences in the azimuth angles of the magnetic lineation with geological time and the site location characterised by approximate longitude of each section using the data given in Table 1. The range of fluctuation of the azimuth of lineation for the sections considered remains essentially same before or after rotation. Also, it is evident that with the exception of the Surai Khola, the longitudinal variations in lineation are more important than the time-dependent ones. Differences of a few degrees in the lineations (corrected for the rotation amount) could be explained by the yet unaccounted differences in the palaeo-north direction which might have varied due to continuing anticlockwise rotation of the Indian plate with respect to Eurasia. As the compression directions are estimated as orthogonal to the lineations corrected for rotation, the same logic applies to them as well. It is supposed here that the N14°E direction of compression obtained by correcting magnetic lineation for remanence-based rotation for the Tinau Khola section, which is one of the best-defined in terms of polarity and magnetic fabric, better fits the general NNE compression direction proposed by other nonmagnetic datasets. Hence, preference is given to the rotated dataset in this paper.

In order to give a better picture of the variations in the angular dataset, the average remanence and compression directions at section level presented in Table 1 are shown in Fig. 5. The data, time-averaged by section, imply that the compression direction in the Himalayan foreland basin remained in general N to NNE with significant deviations (N58°E) in the Amilia–Tui area.

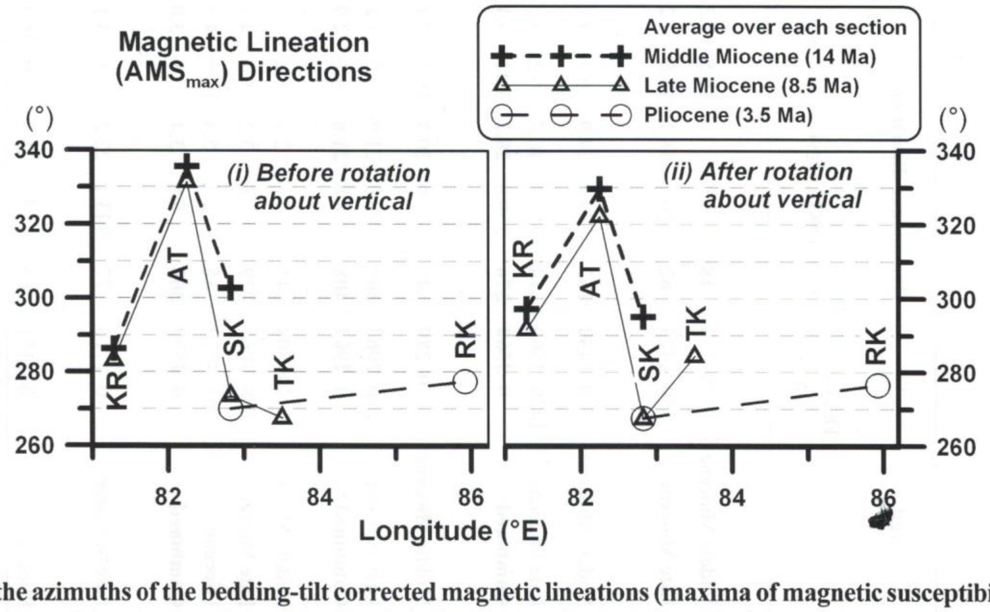

Fig. 4: Plots of the azimuths of the bedding-tilt corrected magnetic lineations (maxima of magnetic susceptibility anisotropy axes) as a function of longitude of the sampling locality and geological age. The times of 14, 8.5, and 3.5 Ma shown correspond approximately to the mid-point of the time span occupied by Middle Miocene, Late Miocene, and Pliocene: (i) before, and (ii) after correction of the directions for the amount of rotation (about vertical) since the acquisition of characteristic remanence derived from magnetic polarity data.

Table 1: Mean remanence, magnetic lineation, rotation about the vertical and inferred compression directions for the Nepalese Siwaliks sections

Section ID	Age	Remanence directions[*]							Magnetic lineations (AMSmax)[**]							Rotation and compression data[***]		
		Thickness, m	N	Decl	Incl	k	α_{95}	±dDecl	N	Trend	Plunge	e	s	k	(Peak-e)/s	Rotation (°) about vertical	Corrected k_{max}	Compre-ssion direction
Khutia (KK)	Middle Miocene	0–530	48	349.4	13	16.5	5.2	5.3								-10.6		
	Late Miocene	530–2423	82	346.8	18.1	14.6	4.2	4.4								-13.2		
Karnali (KR)	Middle Miocene	0–1439	162	349.2	24.9	6.9	4.6	5.1	92	286.4	1.8	4.1	1.37	22.44	20.27	-10.8	297.2	N27E
	Late Miocene	1439–3560	214	351.6	16.7	6.2	4.2	4.4	146	283.2	3.4	4.24	1.41	34.44	24.38	-8.4	291.6	N22E
	Combined	**0–3560**	**376**	**350.6**	**20.2**	**6.42**	**3.1**	**3.3**	**238**	**284.6**	**1.1**	**4.34**	**1.45**	**54.89**	**28.89**	**-9.4**	**294**	**N24E**
Amilia–Tui (AT)	Middle Miocene	0–280	43	6	20.9	10.5	7.1	7.5	124	155.6	0.8	4.2	1.4	29.56	20.27	6	329.6	N60E
	Late Miocene	280–2967	365	9.2	21.9	6.5	3.1	3.3	296	331.4	5.2	4.37	1.46	67.78	17.24	9.2	322.2	N52E
	Combined	**0–2967**	**408**	**8.8**	**21.8**	**6.7**	**2.9**	**3.1**	**420**	**336.4**	**3.4**	**4.41**	**1.47**	**95.33**	**19.84**	**8.8**	**327.6**	**N58E**
Surai (SK)	Middle Miocene	0–508	45	7.6	2.4	5.6	10	9.9	20	302.7	8.3	3.1	1.03	6.44	5.59	7.6	295.1	N25E
	Late Miocene	508–3063	229	6	3.2	5.4	4.4	4.4	199	273.4	6.0	4.31	1.44	46.22	26.46	6	267.4	N3W
	Pliocene	3063–4579	35	2.5	5.8	12.9	4.5	4.5	35	270.0	0.0	3.58	1.19	9.78	8.73	2.5	267.5	N3W
	Combined	**0–4579**	**308**	**5.8**	**3.4**	**0.3**	**3.8**	**3.8**	**49**	**277.4**	**3.8**	**3.8**	**1.27**	**12.89**	**9.81**	**5.8**	**271.6**	**N2E**
Tinau (TK)	Late Miocene	0–1710	77	343.1	22.2	16.4	4.1	4.4	112	267.5	4.6	4.17	1.39	26.89	30.45	-16.9	284.4	N14E
Rato (RK)	Pliocene	0–1151	61	0.8	26.8	9.0	6.4	7.1	49	277.4	3.8	3.8	1.27	12.89	9.81	0.8	276.6	N7E

[*] N is no. of specimens/sampling levels. Decl and Incl correspond to mean bedding-corrected declination and inclination of characteristic depositional remanence, respectively. They are provided with the concentration parameter (k) and the radius of the ellipse at 95% level of confidence (α_{95}). [**] Parameters based on density contouring using the Gaussian smoothing (Robin and Jowett, 1986). e: expected value, s: dispersion, k: counting function. [***] The rotations angles are with respect to geographic north, with negative sign signifying counterclockwise direction. Compression direction is orthogonal to the corrected k_{max} direction (trend of magnetic lineation corrected for the rotation about the vertical).

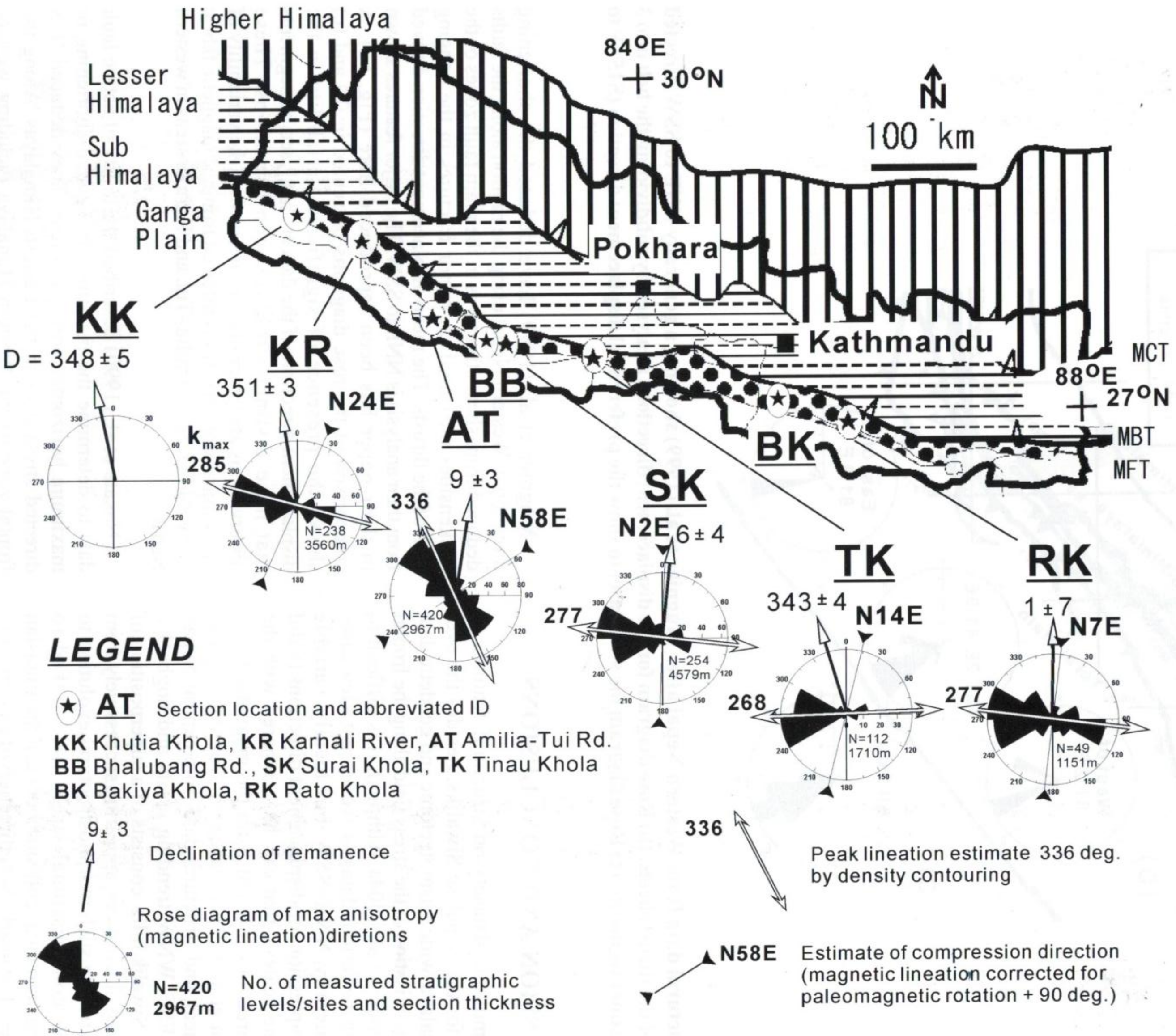

Fig. 5: Geological sketch map of Nepal, showing the locations of sections studied in detail for magnetism. The magnetic lineations are used to determine the compression directions. The magnetic lineations (roses), their best estimate based on density contouring as well as the magnetic declination (D) of the palaeoremanence are given in present-day geographical coordinates. The estimated direction of compression is orthogonal to the magnetic lineation corrected for the angle of rotation shown by the magnetic declination and therefore is relative to the north, which is assumed as fixed during the middle Miocene to Pliocene times.

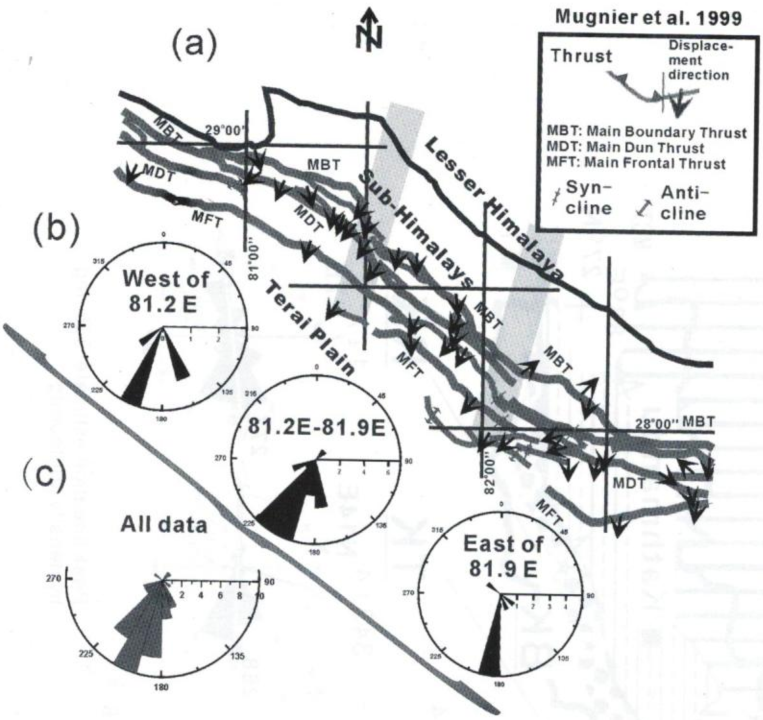

Fig. 6: (a) Structural data from Western Nepal after Mugnier et al. (1999) showing a generally NNE to SSW directed displacement of the thrust sheets. (b) Rose diagram for the displacement directions analysed by subdividing the belt into 3 structurally distinct segments. (c) Rose diagram for all dataset to show the preferential displacement direction (S15°W to S30°W).

DISCUSSION AND CONCLUSIONS

There are multiple datasets on structural features of various scales for the Nepalese Siwaliks, besides the ever increasing Himalaya-wide seismotectonic and geodetic data that allow characterisation of the stress field along the frontal belt (e.g., Bollinger et al. 2004). Although it is difficult to directly compare the various datasets, we present a few cases to show a generally NNE–SSW but locally variable shortening, compression, or displacement directions (valid for various time scales), that can be compared with the compression directions inferred from the magnetic fabric data. Delcaillau et al. (1987), based on sedimentological, geomorphological, and structural data from central Nepal, show that the ESE–WNW trending crests and hogbacks, comprising the Siwalik hills, consists of a superposition of several imbricated thrust slices, appearing successively from N to S. They attribute such morphostructural evolution to the NNE–SSW compressional stress field linked to maintained intracontinental collision between the Eurasian and Indian plates. The nearly N–S direction of compression derived from the analysis of microstructures in Rato Khola (RK) area, in eastern Nepal, close to their Main Siwalik thrusts 1 and 2, is in accord with the compression direction estimated from our magnetic fabric data (cf. Fig. 6 in Delcaillau et al. and Fig. 5 this paper).

Mugnier et al. (1999) have deduced the shortening direction in Western Nepal using the motion along the faults deduced from shear structures in the main fault zones or the slickensides measured on minor fractures in the hanging wall of the thrusts. The mean displacement direction derived from their analysis is NNE to SSW. The major features shown in their paper has been reproduced here (Fig. 6a). A comparison of the rose diagrams presented in (b) and (c) shows the presence of significant variability in the displacement directions if the data are analysed by segments that have distinct structural configurations. These observations are generally consistent with the variability of the compression directions inferred from the magnetic fabric in the Surai Khola, Amilia–Tui, and Karnali areas in western Nepal.

Nakata et al. (1990) described the utility of active fault data to determine the maximum horizontal shortening or maximum horizontal principal stress. They deduced N–S directed stress axes in the Eastern Himalayas. Along the frontal zone of the Western Himalaya including western Nepal, however, the stress direction was found to change gradually from N–S to NE–SW direction. These inferences are likely to be valid for the order of 10,000 year as implied by the term "active".

According to Bettinelli et al. (2006), the geodetic data are consistent with models that assume the average displacements to be parallel to the direction of convergence along N23°E in central and eastern Nepal, but N30°E in western Nepal.

Magnetic fabric in the Siwaliks is well defined, and it can be easily measured in the same samples as those used for magnetostratigraphy. There is good parallelism among the magnetic lineation-based compression direction, displacement directions based on microstructures, and fault-plane solutions as well as GPS based displacement directions from the various segments of the Himalayan foreland basin.

In this study, it has been explicitly assumed that lineation development preceded rotation. If the tectonic rotation and the finite strain producing the horizontal component of anisotropy were synchronous over the time since deposition, it is likely that the amount of rotation derived probably is an overestimate of the net rotation of the AMS vector from its original position. Another point worthy to consider is the extent to which the temporal variations are averaged out or underestimated due to the differences in the integral time (age span) of the various sections. Although much remains to be yet tested, the emphasis in this paper has been to present magnetic fabric data in such a way that they could be used for structural interpretation, especially in relation to a compression regime. The advantage of a combined palaeomagnetic and rockmagnetic (magnetic fabric) approach is the ability to provide compression-related directions in relation to the geological age spanning at least for the last 16 Ma for the foreland basin considered.

ACKNOWLEDGEMENTS

This study is based on numerous data on magnetic polarity stratigraphy and magnetic fabric generated under several research projects of Erwin Appel and Wolfgang Rösler (University of Tuebingen, Germany), with whom the author has collaborated on several occasions. The original manuscript and its revised version benefited very much by critical as well as constructive reviews of Craig Zones. The author would like to acknowledge a JSPS Grant-in-aid for scientific research (kiban kenkyú C, No. 17540427), an affiliation with the 21st Century COE Programme for Neo-Science of Natural History (Leader: Professor Dr. H. Okada) at Hokkaido University, Sapporo, Japan, as well as the organisers at DMG Nepal for organising the Seismotectonics Workshop 2006.

REFERENCES

Appel, E., Rösler, W. and Corvinus, G., 1991, Magnetostratigraphy of the Miocene–Pleistocene Surai Khola Siwaliks in west Nepal. Geophys. Jour. Int., v. 105, pp. 191–198.

Bettinelli, P., Avouac, J-P., Flouzat, M., Jouanne, F., Bollinger, L., Willis, P. and Chitrakar G. R., 2006, Plate motion of India and interseismic strain in the Nepal Himalaya from GPS and DORIS measurements. Jour. Geod., v. 80 (8–11), pp. 567–589.

Bollinger, L., Avouac, J., Cattin, R., and Pandey, M. R., 2004, Stress buildup in the Himalayas. Jour. Geophys. Res., v. 109, B11405, doi:10.1029/2003JB002911.

Cande, S. C. and Kent, D. V., 1995, Revised calibration of the geomagnetic polarity timescale for the Late Cretaceous and Cenozoic. Jour. Geophys. Res., v. 100, pp. 6093–6095.

DeCelles, P. G., Gehrels, G. E., Quade, J., Ojha, T. P., Kapp, P. A. and Upreti, B. N., 1998, Neogene foreland basin deposits, erosional unroofing, and the kinematic history of the Himalayan fold-thrust belt, western Nepal. Geol. Soc. Am. Bull., v. 110(1), pp. 2–21.

Delcaillau, B., Hérail, G. and Mascle, G., 1987, Evolution géomorphostructurale de fronts de chevauchement actifs: le cas des chevauchements intrasiwaliks du Népal central. Zeitschrift für Geomorphologie Neue Forschung, v. 31, pp. 339–360.

Dhital, M. R., Gajurel, A. P., Pathak, D., Paudel, L. P. and Kizaki, K., 1995, Geology and structure of the Siwaliks and Lesser Himalaya in the Surai Khola–Bardanda area, mid Western Nepal. Bull. Dept. Geol., Tribhuvan Univ., 4, pp. 1–70.

Gautam, P. and Appel, E., 1994, Magnetic-polarity stratigraphy of Siwalik Group sediments of Tinau Khola section in west central Nepal, revisited, Geophys. Jour. Int., v. 117, 223–234.

Gautam, P. and Fujiwara Y., 2000, Magnetic polarity stratigraphy of Siwalik Group sediments of Karnali River section in western Nepal. Geophys. Jour. Int. 142, pp. 812–824.

Gautam, P. and Pant, S. R., 1996, Magnetic fabric of Siwalik Group sediments of Tinau Khola section, west central Nepal. Bull. Dept. Geol., Tribhuvan Univ., v. 5, pp. 21–36.

Gautam, P. and Rösler W., 1999, Depositional chronology and fabric of Siwalik group sediments in Central Nepal from magnetostratigraphy and magnetic anisotropy. Jour. Asian Earth Sciences, v. 17, pp. 659–682.

Gautam, P., Hosoi A., Regmi K. R., Khadka, D. R. and Fujiwara, Y., 2000, Magnetic minerals and magnetic properties of the Siwalik Group sediments of the Karnali River section in Nepal. Earth Planets Space, v. 52, pp. 337–345.

Harrison, T. M., Copeland, P., Hall, S. A., Quade, J., Burner, S., Ojha, T. P., and Kidd, W.S.F., 1993, Isotopic preservation of Himalayan/Tibetan uplift, denudation, and climatic histories in two molasse deposits. Jour. Geol., v. 101, pp. 157–175.

Hoorn, C., Ohja, T., and Quade, J., 2000, Palynological evidence for vegetation development and climatic change in the sub-Himalayan zone (Neogene, Central Nepal), Palaeoclim., Palaeogeogr., Palaeoecol., v. 163, pp. 133–161.

Huyghe, P., Mugnier, J-L. Gajurel, A. P., and Delcaillau, B., 2005, Tectonic and climatic control of the changes in the sedimentary record of the Karnali River section (Siwaliks of western Nepal). The Island Arc, v. 14, 311–327.

Jelinek, V., 1981, Characterization of magnetic fabric of rocks. Tectonophysics, v. 79, pp. 563–567.

Johnson, N. M., Opdyke, N. D., Johnson, G. D., Lindsay, E. H. and Tahirkheli, R. A. K., 1982, Magnetic polarity stratigraphy and ages of Siwalik group rocks of the Potwar plateau, Pakistan. Palaeogeogr., Palaeoclimatol., Palaeoecol., v. 37(1), pp. 17–42.

Lee, T. Q., Kissel, C., Laj, C., Horng, C. S., and Lue, Y. T., 1990, Magnetic fabric analysis of the Plio–Pleistocene sedimentary formations of the Coastal Range of Taiwan, Earth Planet Sci. Lett., v. 98, pp. 23–32,

Molnar, P., 2005, Mio–Pliocene Growth of the Tibetan Plateau and Evolution of East Asian Climate, Palaeontologia Electronica v. 8(1), 2A:23 p.

Mugnier, J. L., Leturmy, P., Mascle, G., Huyghe, P., Chalaron, E., Vidal, G., Husson, L. and Delcaillau, B., 1999. The Siwaliks of western Nepal: I. Geometry and kinematics, Jour. Asian Earth Sciences, v. 17(5-6), 1999, pp. 629-642.

Nakata, T., Otsuki, K. and Khan, S. H., 1990, Active faults, stress field, ad plate motion along the Indo-Eurasian plate boundary. Tectonophysics, v. 181, pp. 83–95.

Nakayama, K. and Ulak, P. D., 1999, Evolution of fluvial style in the Siwalik Group in the foothills of the Nepal Himalaya. Sedimentary Geology, v. 125, pp. 205–224.

Ojha, T. P., Butler, R. F., and Quade, J., 2000. Magnetic polarity stratigraphy of the Neogene Siwalik Group at Khutia Khola, far western Nepal. Geol. Soc. America Bull., v. 112, pp. 424–434.

Robin, P.-Y. F. and Jowett, E. C., 1986, Computerized density contouring and statistical evaluation of orientation data using counting circles and continuous weighting functions. Tectonophysics, 121, 207–223.

Robion P., Grelaud, S., de Lamotte D. F., 2007, Pre-folding magnetic fabrics in fold-and-thrust belts: Why the apparent internal deformation of the sedimentary rocks from the Minervois basin (NE – Pyrenees, France) is so high compared to the Potwar basin (SW – Himalaya, Pakistan)? Sedimentary Geology, 196, 181–200.

Rochette, P., Jackson, J. and Aubourg, C., 1992, Rock magnetism and the interpretation of ansisotropy of magnetic susceptibility. Rev. Geophys., 30(3), 209–226.

Rösler, W. and Appel, E., 1998. Fidelity and time resolution of the magnetostratigraphic record in Siwalik sediments: high-resolution study of a complete polarity transition and evidence for cryptochrons in a Miocene fluviatile section, Geophys. Jour. Int., v. 135, pp. 861–875.

Rösler, W., Metzler, W. and Appel, E., 1997, Neogene magnetic polarity stratigraphy of some fluviatile Siwalik sections, Nepal, Geophys. Jour. Int., v. 130, 89–111.

Sagnotti, L., Winkler A., Montone P. et al., 1999, Magnetic anisotropy of Plio–Pleistocene sediments from the Adriatic margin of the northern Apennines (Italy): implications for the time-space evolution of the stress field, Tectonophysics, v. 311, pp. 139–153.

Tanaka, S., 1997, Uplift of the Himalaya and climatic. change at 10 Ma – Evidence from records of carbon stable isotopes and fluvial sediments in the Churia Group, central. Nepal. Jour. Geol. Soc. Japan, 103 (3), 253–264

Tokuoka, T., Takayasu, K., Hisatomi, K., Yamasaki, H., Tanaka, S., Konomatsu, M., Sah, R. B. and Rai, S. M., 1990. Stratigraphy and geologic structures of the Churia (Siwalik) Group in the Tinau Khola–Binai Khola area, West Central Nepal. Mem. Fac. Sci., Shimane Univ. 24, 71–88.

Tokuoka, T., Takayasu, K., Yoshida, M. and Hisatomi, K., 1986, The Churia (Siwalik) Group of the Arung Khola area, West Central Nepal, Mem. Fac. Sci., Shimane Univ., v. 20, pp. 135–210.

Ulak, P. D. and Nakayama, K., 2001, Neogene fluvial systems in the Siwalik Group along the Tinau Khola section, West Central Nepal Himalaya. Jour. Nepal. Geol. Soc., v. 25, pp. 111–122.